

Introduction

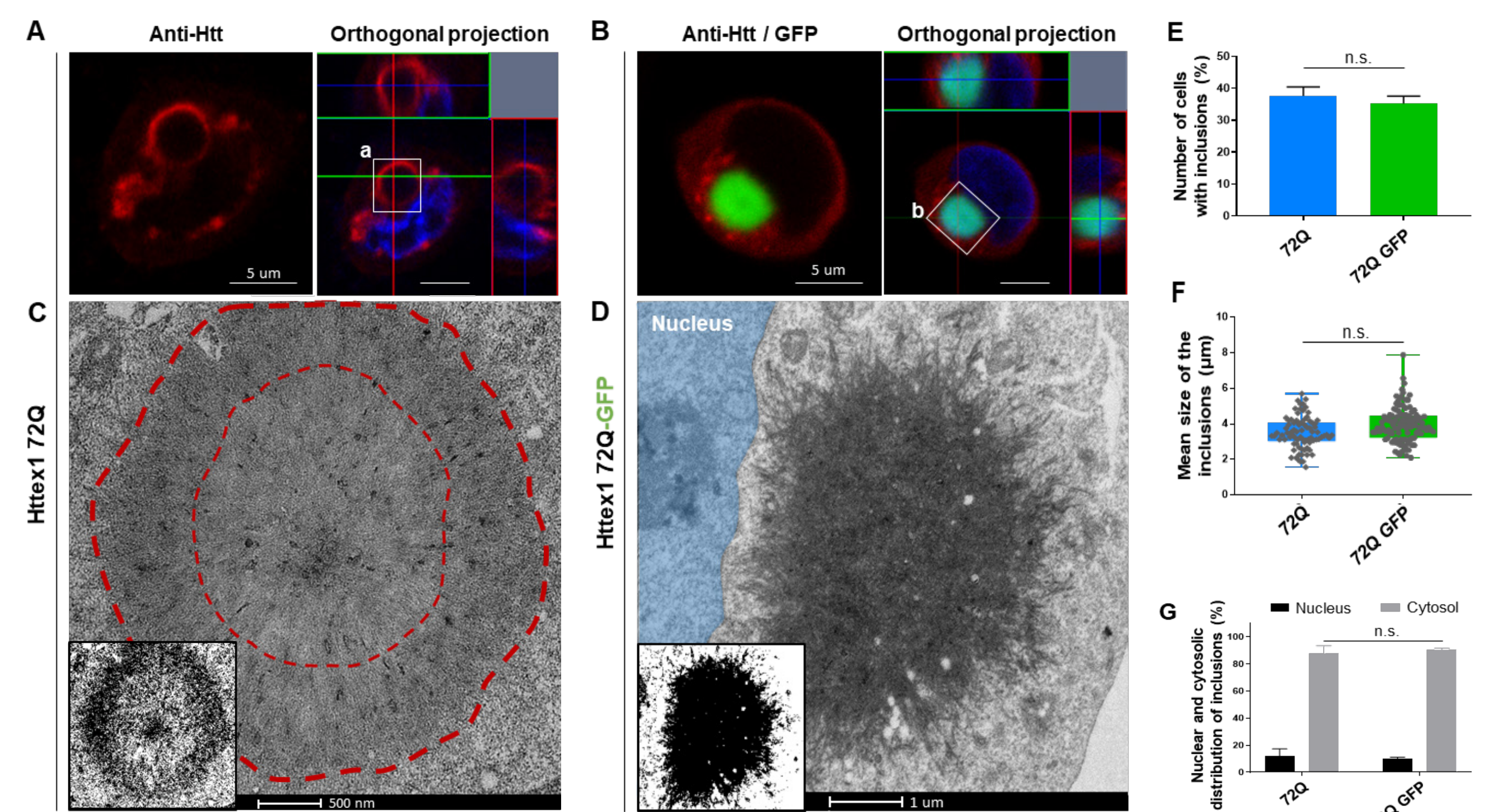
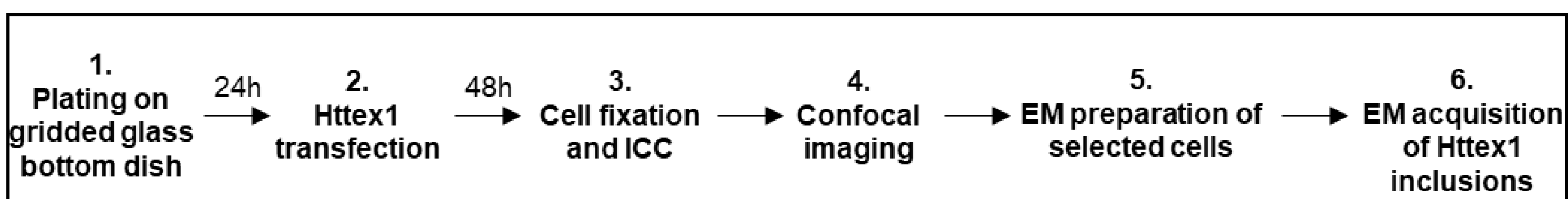
Background: Despite the identification of the gene and mutations that cause Huntington's Disease (HD) and the strong evidence linking the aggregation of the Huntingtin protein (Htt) to the pathogenesis of the disease, the molecular mechanisms underlying Htt aggregation and neurodegeneration remain poorly understood. This is in part due to the lack of disease models that reproduce the biochemical, structural and pathological diversity of HD pathology in humans. Although fluorescent protein, such as GFP, are commonly used to allow direct monitoring of Htt aggregation, the extent to which these large proteins influence the aggregation and structural properties of Htt inclusions has never been investigated.

Goal: To develop cellular models that reproduce HD pathology at the biochemical and structural levels.

Methods: Herein, we applied an imaging-based approach using confocal imaging and correlative light electron microscopy (CLEM) to investigate the aggregation properties of Htt exon1 bearing different polyQ length fused or not to eGFP at the C-terminus.

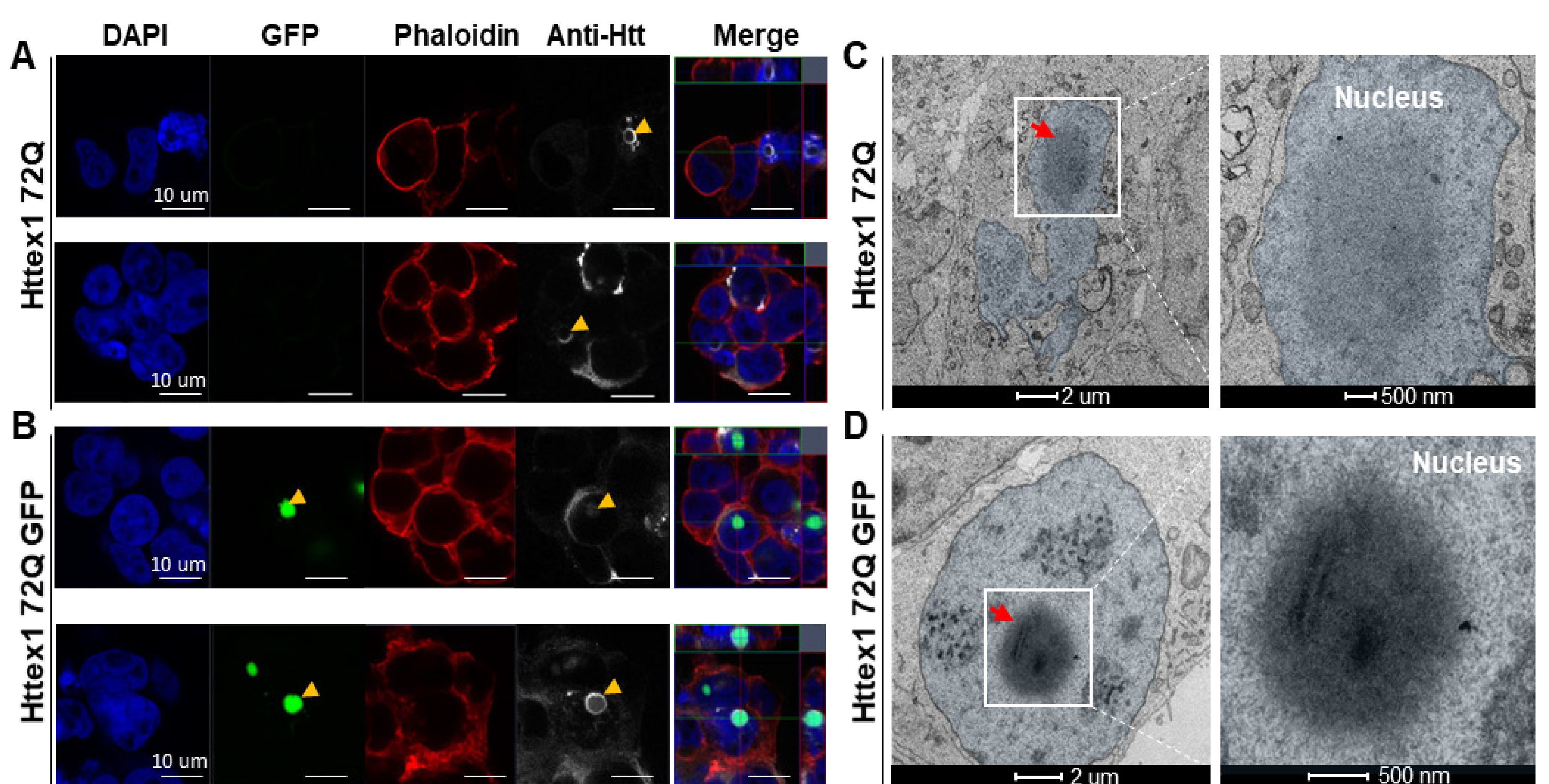
Results

CLEM reveals a striking structure and morphological features between cytoplasmic Httex1 72Q inclusions produced in the presence or in the absence of a GFP tag



Confocal images of **A.** Httex1 72Q and **B.** Httex1 72Q GFP, 48h after transfection. Httex1 expression (red) was detected using a specific primary antibody against the N-terminal part of Htt and the nucleus was stained with DAPI (blue). Electron micrographs of **C.** Httex1 72Q and **D.** Httex1 72Q GFP inclusions corresponding to confocal images panel A, and B (white square) respectively. Add-in binary images generated from electron micrographs by median filtering and Otsu intensity threshold. **E.** Percentage of cells containing inclusions 48h after overexpression of Httex1 72Q (+/-GFP). **F.** Mean size of the inclusions. **G.** Nuclear and cytosolic distribution. A total of 193 inclusions were counted and measured using FIJI over 3 different experiments including 3 imaging fields per condition. Quantitative confocal imaging did not show any differences between cytoplasmic Httex1 72Q inclusions.

CLEM reveals different structural and morphological features between the cytoplasmic and nuclear tag-free Httex1 inclusions but not for Httex1 72Q-GFP



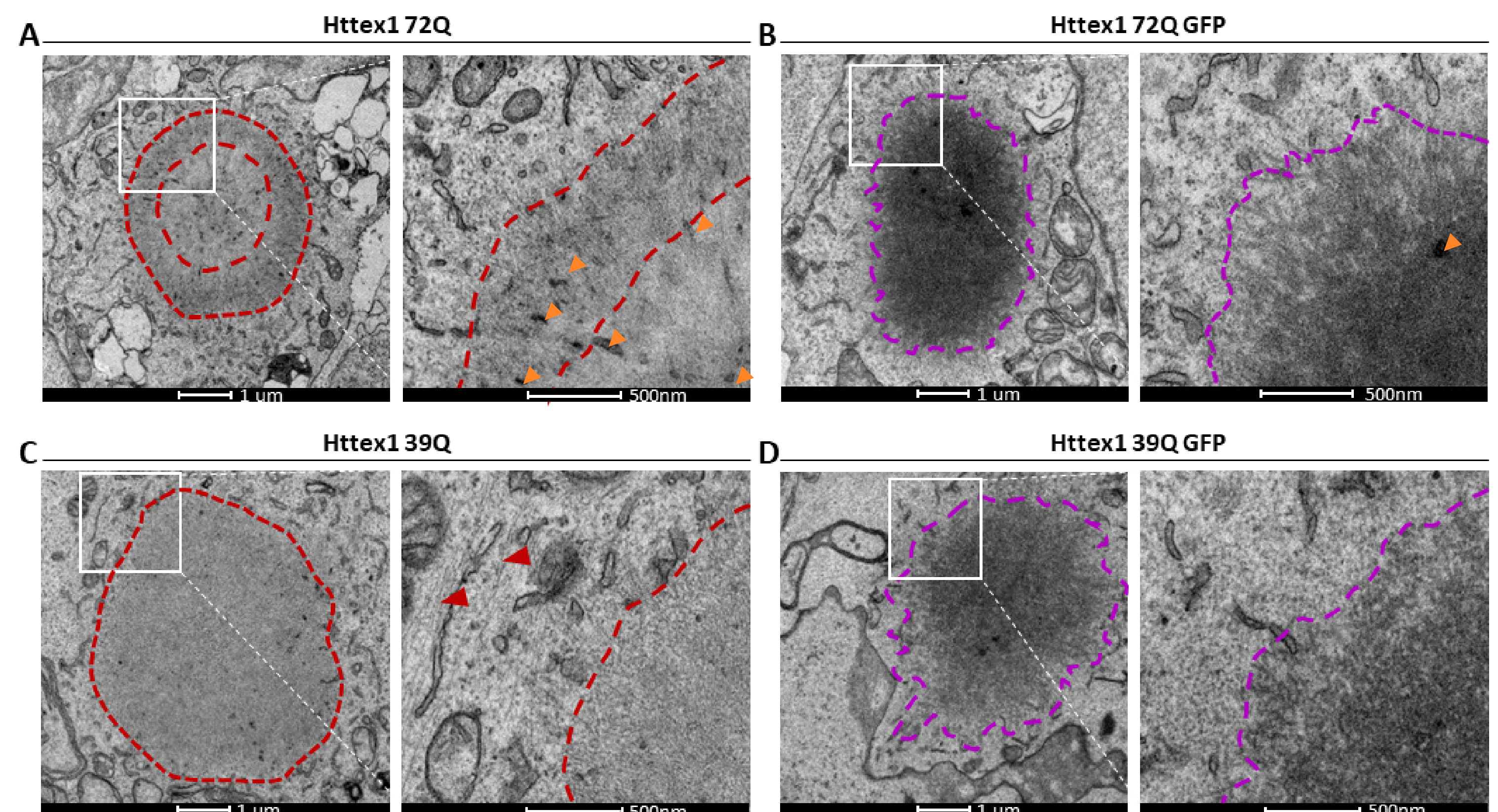
Representative confocal images of **A.** Httex1 72Q and **B.** Httex1 72Q GFP nuclear aggregates, 48h after transfection. Httex1 expression (grey) was detected using a primary antibody against the N-terminal part of Htt (2B7 or Ab109115). The nucleus was stained with DAPI (blue) and Phalloidin (red) used to stain the actin F. Yellow arrowheads indicate Httex1 nuclear aggregates. Electron micrographs of nuclear aggregates of **C.** Httex1 72Q and **D.** Httex1 72Q GFP.

Acknowledgements:

- We thank Dr. Arne Seitz and his staff at the Biop (EPFL) for their support, Dr. Romain Guiet and Olivier Burri for the confocal imaging.
- We are grateful to Mr Driss Boudeffa and Mr Ricci Jonathan for their continuous technical assistance.
- We thank the CIME for the use of their equipments and continuous support
- This project was supported by the CHDI foundation.

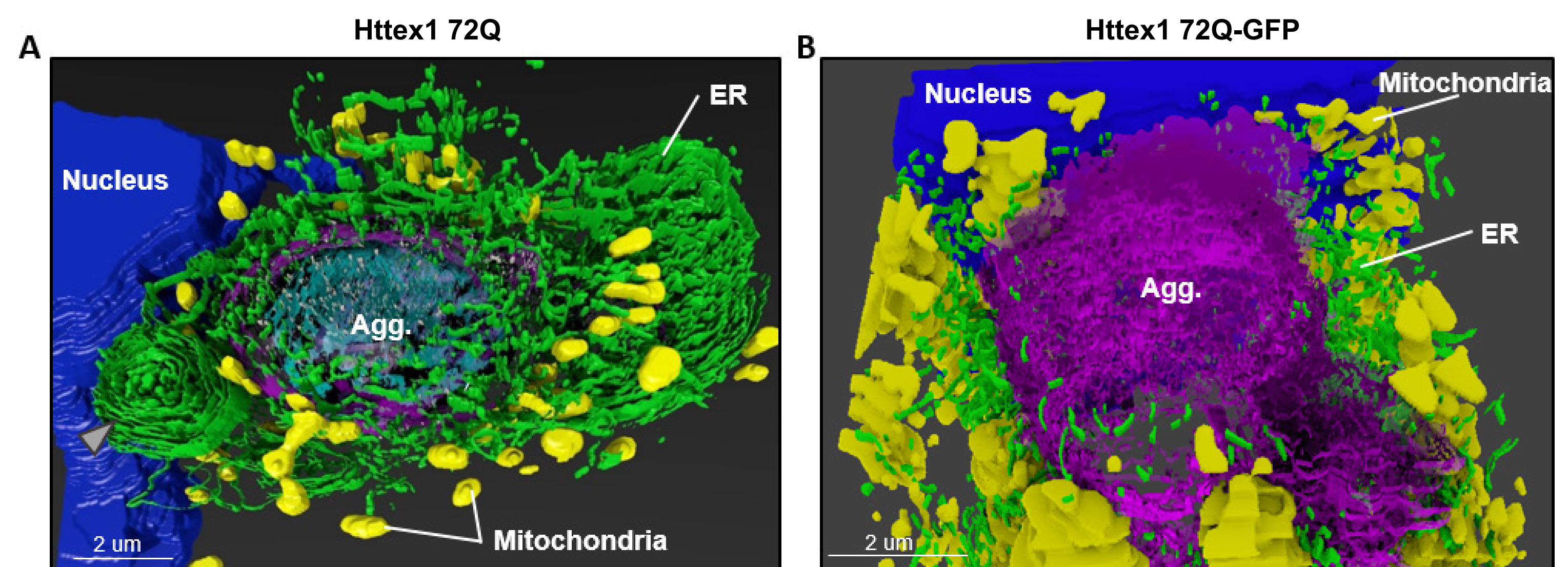


The length of the polyQ repeats influences the structural properties and organization of Httex1 inclusions with or without GFP



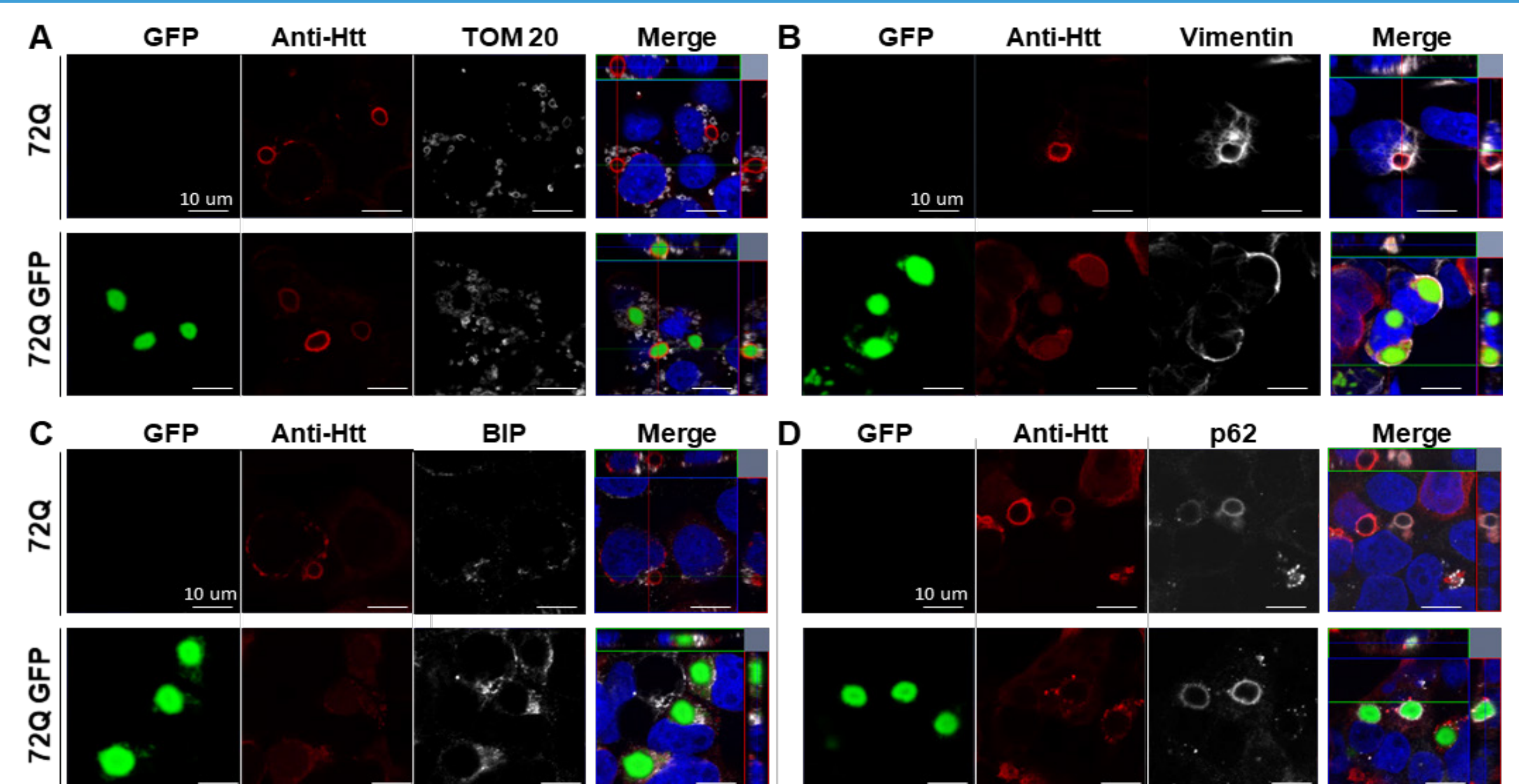
Representative electron micrographs and higher magnification of cellular inclusions 48h after transfection in HEK cells; **(A)** Httex1 72Q, **(B)** Httex1 72Q-GFP, **(C)** Httex1 39Q and **(D)** Httex1 39Q-GFP. Dash-lines represent the edge of the inclusions and the interface between the core and the shell for Httex1 72Q. Orange arrowheads indicate ER-derived membranous structures. Red arrowheads indicate fibrils outside of the Httex1 inclusion.

EM-based 3D reconstructions of Httex1 inclusions revealed recruitment of membranous structures and significant ER disruption mostly for Httex1 72Q



A. Httex1 72Q cellular inclusion. **B.** Httex1 72Q-GFP cellular inclusion. Httex1 inclusion (purple), aggregate core (cyan), ER membranes (green), intra-aggregate membranous structures (white) nucleus (blue) and mitochondria (yellow). Formation of stacked ER cisternae close to Httex1 inclusion is highlighted by grey arrowhead.

Aggresome markers in addition to mitochondria and ER are found in periphery to Httex1 inclusions



Representative confocal images of Httex1 72Q(+/-GFP) inclusions 48h post transfection. The nucleus was stained with DAPI (blue), Httex1 with MAB5492 primary antibody, mitochondria using anti-TOM 20 primary antibody **(A)**, Aggresome intermediate filament using anti-Vimentin primary antibody **(B)**, ER using anti-BIP primary antibody **(C)**, and the autophagolysosomes using anti-p62 primary antibody **(D)**.

Conclusions

- Comparative analysis at the resolutions obtained by standard confocal imaging did not reveal significant differences in the number, size and subcellular localization, of Httex1 aggregates with or without a GFP tag.
- Using high-resolution techniques with Electron Microscopy (EM) approaches we could demonstrate that the cellular aggregates formed by mutant Httex1 72Q-GFP do not reproduce many of the structural and organizational features of Httex1 inclusions formed by tag-free mutant Httex1 72Q.
- Cytoplasmic and nuclear Htt inclusions exhibit distinct ultrastructural properties
- Electron micrographs reveal that cytoplasmic Httex1 39Q inclusions are less mature compared to Httex1 72Q, suggesting that the polyQ domain plays a dominant role in regulating the formation and ultrastructure properties of the Httex1 inclusions.

Altogether, our studies provide novel insight into the mechanisms of Htt aggregation and inclusion formation and caution against the use of fluorescent protein tags without systematic analysis of their effect on the cellular properties of Htt proteins.